RSC Advances

ROYAL SOCIETY OF CHEMISTRY

www.rsc.org/advances

Gamma Irradiation Studies of Composite Thin Films of Poly Vinyl Alcohol and Coumarin

Feroz A. Mir[1,ϕ,*], Adil Gani [2]and K.Asokan[3]

[1] *University Science Instrumentation Centre (USIC), University of Kashmir, Srinagar-190006, J&K India.*

[2] *Department of Food Science & Technology, University of Kashmir, Srinagar-190006, J&K, India.*

[3]*Materials Science Division, Inter University Accelerator Centre, Aruna Asaf Ali Marg, New Delhi 110067, India*

Abstract

Composite films of Imperatorin (a coumarin molecule) and Poly Vinyl Alcohol (PVA) are prepared by solution casting method. These composite films are exposed to γ-radiation of different doses at room temperature. These composite films are characterized by X-ray diffraction (XRD), Fourier Transform infrared (FT-IR), UV-Visible and dielectric spectroscopy. After doping, XRD data shows semicrystalline to amorphous phase formation in the PVA back bone. FT-IR analysis of these composite films show various bands and a significant impact on them can be observed after irradiation. UV-Visible spectroscopy of these composite films shows various absorption bands. But the absorption band at 311 nm is the sharpest one. In these films, the optical band gap is determined by using Tauc's plots. These films follow indirect allowed transitions. In the present samples, the optical band gap increases with irradiation and finally decreases at highest dose. The Urbach energy also decreases with increasing radiation dose, and gives clear indication that radiation induced defects are formed in the system. Additionally, both dielectric constant and loss changes with radiation dose. These changes are explained based on universal dielectric response (UDR) model and which also supports disorderness in the system.

Keywords: composite film, dielectric, gamma radiation, UV-Vis, FITR,dielectric spectroscopy.

*****Corresponding author : Dr. Feroz A. Mir*

ϕ Presently working at Department of Nuclear Medicine, Sher-i-Kashmir Institute of Medical Sciences, Srinagar-190011, J&K, India.

Tel.No: +19 9858338012, Email: shaheen.mir2013@gmail.com, famirnit@gmail.com

I. Introduction

Chromatic organic dyes are vividly investigated and used as potential chemical dosimeters [1]. These compounds are utilized, either in the liquid or aqueous form, and or embedded in various suitable polymeric matrixes or films [1-5]. Different kinds of polymeric films are used for measuring and tracking of ionizing photons and electrons. These radiochromic thin films are also used as 3D dosimeters. These films have wide application in radiation processing, and routine dose control for different kinds of ionization irradiation. The fabrication of various types of films (or polymers matrixes) is a continuous effort to develop more reliable, stable, simpler and cheaper system for routine dosimetery. Therefore, these efforts also led to the successful development of some polymer (e.g. cellulose triacetate.) films or foils, and are simply analyzed with the help of UV spectrophotometer.

Polyvinyl alcohol (PVA) with a general formula $[-CH_2CH(OH)-]_n$ is a well-known polymer for many technological applications since it forms a film with high transparency, very good flexibility and wide commercial availability. The exposure of polymer materials to ionizing radiations such as γ-rays produce changes in the microstructural properties of the material as a result of inducing structural defects, which in turn affect the optical properties [6]. These changes are strongly depending on the internal structure of the material, the radiation energy and the irradiation dose. Clarification of these changes is quite significant, not only to recognize the physicochemical functions and spectroscopic properties of these materials, but also to increase their applicability in different fields and enable information about the induced irradiation defects and their interaction with the matter compositions [7].The effect of ionization radiations on various type dye molecules in non-aqueous solvents and in some polymeric films are already discussed in literature [7-12]. For most of these composites, a linear dose response curves were

obtained over larger dose range. The observed properties shown by these dyes, projects their possible use as chemical dosimeters within that linear dose range. Other various polymeric films coated with some suitable dyes have also been investigated for chemical dosimetery [7-12].

Coumarins are among the important group of naturally occurring compounds largely extracted from the plants and are also produced artificially [13]. Since decades these Coumarins are studied for their various applications [13]. From last seventies, aqueous coumarin solutions are used for dose evaluation of different types ionization radiations [14-18]. Recently, highly sensitive fluorescent dosimeters made up of coumarin derivatives and other dyes were studied [14-18]. To enhance their various properties, coumarins and their derivatives are isolated from selected plants or prepared and then modified as per the requirements [13].

In our previous studies on different coumarins, we investigated the effect of γ-radiation on their optical properties [19-20]. In these studies, their possible uses as dosimeters in the low radiation zone were projected. These studies motivated us to investigate the effect of γ-radiation on various physical properties of some selected isolated plant molecule embedded in polymer matrix. Therefore current study focuses on the effect of γ-radiation on different properties of composites films of Imperatorin (a coumarian molecule) and PVA .

2. Material and Methods

The compound Imperatorin having molecular formula $C_{16}H_{14}O_5$, and molecular mass 286 was isolated from ethyl acetate extract of the roots of the plant Prangos pabularia by column chromatography, using silica gel as adsorbent. The structure and other characterizations of this compound are already published elsewhere [21-22]. To prepare polymer composite film of this compound, 13.813mg of Imperatorin (or $C_{16}H_{14}O_5$) was dissolved in 35ml of ethanol (as solution I). In the another beaker (as solution II), 5gms of PVA with molecular weight (60,000-12,5000)

was mixed in 100 ml of deionized water at 80^{o}C with constant stirring for 3 hour. Here, 5ml, and 15ml of solution I was added to 25ml each of solution II. Then these composite solutions were mixed for 1 hour with constant stirring at 75 ^{o}C. These composite gels were further thoroughly mixed and placed in an ultrasound bath (at 30 kHz frequency, power 50Watts) for 5 minutes to remove the formed bubbles (if any). Finally, these gels were poured into Petri dishes and dried for three days. After three days, these films were peeled off from the dishes (packed in black paper sheets; to avoid exposure of light) for further characterizations and study. For the irradiation studies, only low doped (5ml added) films were irradiated with ^{137}Cs γ-radiation source (γ-ray energy = 662 keV with activity 703.45 cGy/min), the facility available at Sher-i-Kashmir Institute of Medical Sciences, Srinagar, Jammu & Kashmir, India in dose range 0-50Gy (with doses 15,20, 30, and 50 Gy). These films were characterized by powder x-ray diffraction (XRD) by using Bruker D8 x-ray diffractometer with Cu K_{α} radiation. Attenuated Total reflection (ATR) Fourier transform infrared (FTIR) spectroscopy of these films were studied from 650-4000cm^{-1} wavelength range by Agilent Cary 630 spectrometer. Ultraviolet–visible (Uv-Vis) spectroscopy of unirradiated and irradiated films were recorded on dual beam photospectrometer (Shimadzu UV-1601). The dielectric studies of these films were carried out by parallel plate geometry method (by sputtering gold contacts on both sides of films) in the frequencies 120 Hz–500kHz, using with an Agilent 4285A precision LCR meter. All the experiments were done at normal temperature and pressure (NTP).

3. RESULTS AND DISCUSSION

3.1 XRD studies

Fig.1 shows the XRD pattern of pure PVA, 5ml (added compound) , and 15ml (added compound) added composite films. In pure PVA, a characteristic PVA XRD peak at 2Θ= 19.79^{o}

is observed [23]. It can be noticed that with doping, no peaks of compound are seen separately [21]. However, we observed that the semicrystalline nature of PVA is loss with doping. The apparent reduction of PVA characteristic peak height or broadening with increasing doping can be attributed to the polymer complex formation which leads to polymer chain separation followed by the structure rearrangement. This in turns results in a decrease of the degree of crystallization of PVA. Also, in our doping molecule, there are hydrogen and oxygen atoms, they can interact (via van der Waal's or weak interaction) with hydrogen atoms of PVA matrix. This breaking of semicrystalline nature into purely amorphous may be due to the thermally induced changes in the polymer bonding (as the sample preparation temperature is 75^{o}C) [23]. Further, when heat energy is given to the crystalline region, the lattice start vibrating via phonons and this interaction may lead to the bond breaking or formation new bonds in the system [23]. This feature of interaction in the present case is seen in the crystalline region of host PVA, which shows a drastic decrease in crystallinity. This type of trend was also observed in dye doped PVA [23]. Furthermore, this interaction is also supported by FT-IR data and is described in next section. This observed amorphous nature with heavy doping also led us to focus our study of γ-radiation to low (5ml added compound) doped samples. In addition, XRD pattern of γ-radiation films did not show any significant change and are hence skipped for any further discussions in the current study.

3.2 FT-IR studies

The FT-IR spectra of pure PVA polymer, $C_{16}H_{14}O_4$, and PVA/$C_{16}H_{14}O_4$ composite (with different doping concentrations) are shown in Fig.2. The band at 937 cm^{-1} indicates the presence of chain like structure of PVA [24], suggesting the regular inter-chain bridging in a layer structure through sequential distribution of OH groups, conferring the H-bonding functionality to

planar geometry in the polymer backbone. However, decrease in intensity of this band with increasing concentration of $C_{16}H_{14}O_4$ gives a clear indication of change or alteration to such planer structure, causing strong delocalization of π-electrons, and hence leads to impact various physical properties of polymer [24-25]. The important bands of PVA for different vibrational modes are shown in Fig.2 and are also given in Table I. From the FT-IR spectrum of imperatorin (shown in Fig.2), a strong intensity band at around 1722 cm^{-1} is due to α, β-unsaturated-δ-lactone, bands at around 1586 & 1401 cm^{-1} are due the presence of aromatic moiety, and bands at 1383, 1295 cm^{-1} are because of gemdimethyl [21]. Some important bands of $C_{16}H_{14}O_4$, corresponding to their vibrational modes are also given in Table I. Looking at the spectra of PVA/$C_{16}H_{14}O_4$ composite films (Fig.2), a dramatic change in PVA structure can be observed after doping. In the spectra of PVA/$C_{16}H_{14}O_4$, various bands of filler ($C_{16}H_{14}O_4$) along with the bands of polymer are seen (Fig. 2). However, in these observed bands, shifting with change in intensities are observed.

The broad band at 3280 cm^{-1} due to O-H stretching vibration and band due to O-H vibration of PVA start broadening and sharpening. This could be due to the electrostatic interaction between the aromatic C–H stretching of $C_{16}H_{14}O_4$ and OH electric dipoles in the polymer chain. However, with increase in doping, a reduction in the intensity of band involved in H-bonding within PVA chain (3700-3000 cm^{-1}) is observed. Also, a blue shift of the band at 2920 cm^{-1} (CH asymmetric vibration) is observed. The change seen in these two important regions are corresponding to the formation of hydrogen bonds between the PVA chain and doping molecule. The shifting, change in intensity, and merging of C=O stretching band at 1650 cm^{-1} of PVA and 1715 cm^{-1} corresponding to C=O stretching of the carbonyl of $C_{16}H_{14}O_4$. This also indicates that hydrogen bonds of $C_{16}H_{14}O_4$ are interacting with the hydrogen bonds of

PVA. More precisely here, peak shift demonstrates a strong interaction between PVA and $C_{16}H_{14}O_4$, and giving rise to the localization effects [24]. Moreover, the stretching vibrations of C=C bonds in the aromatic ring, and the deformation vibrations of C–H bonds in CH_2 and CH_3 groups (and aromatic CH groups of compound), are also clearly distinguished in the spectrum [25]. More precisely, the observed bands of PVA /$C_{16}H_{14}O_4$ composites are given in Table I. This alteration of PVA structure with doping is quite consistent with XRD data of these samples.

After exposure to γ-radiations, the spectrum shows changes in various observed bands of PVA /$C_{16}H_{14}O_4$ composites (see Fig. 3). The changes in number, frequency, intensity, and width of the FTIR bands in the particular region of O-H vibrations (3000-3700 cm^{-1}), C-H vibrations (1500–1300 cm^{-1}) and C-O vibrations (1200–1000 cm^{-1}) are related to changes in the conformation and short range interactions of the composite. After irradiations, the changes in intensity of these bands are strongly associated with the changes in the macromolecular structure [24-27]. This observation demonstrates the destruction of C–OH and C–H bonds and possibility of formation of ketones and/or enols [26-27]. The major attention was focused on the bands in the 1160–1010 cm^{-1} region because the absorbance pattern due to ring vibrations in this spectral range is known to be individual for each carbohydrate structures. Also the changes in intensity of bands in region 1200-1500 cm^{-1} indicates the decoupling between OH and CH vibrations due to electrostatic interaction between OH and filler molecules after radiation exposure. In addition, the peak broadening might be attributed to the variations in the π-conjugation length of the PVA chain, which is associated with π-electron delocalization [24-27].The optical and dielectric properties of these irradiated films are also changed exactly as per the FT-IR data and will be discussed in the later sections.

After γ-ray exposure, the ester linkage may have broken down and probably ester radicals have been formed. These ester radicals might result in the release of CO_2, and thus leading to the formation of oxygen radicals. The oxygen radicals once formed can easily be pick up by hydrogen radicals (which are formed due to broken of C−H bonds) and could have formed ketones or phenols [25-27]. The formation of conjugated double bonds or trapped free radicals and ions along degradation mechanism or scheme are already explained by γ- irradiations [24-27]. This process yields either a separation of the oxygen atom or a different substitution of the C atom of the carbonyl moiety with a C=C double bond or a hydrogen atom on one branch. This is likely to cause, either reduction in intensity or a shift of the carbonyl stretching mode [24-27].

3.3 Optical studies

Inset of Fig.4 shows UV-VIS absorption spectra of PVA, $C_{16}H_{14}O_4$, and different doping concentrations of $C_{16}H_{14}O_4$ in PVA films. In the pure PVA film, an absorption band at about 276 nm is observed, and this is due to the π– π* electronic transition [24]. The doping or filler molecule ($C_{16}H_{14}O_4$) shows electronic transitions at 219, 255, 268 and 300 nm. However, in the composite form, these bands are shifted 223, 250, 260, and 311nm. This also indicates the strong interactions going in PVA structure after doping. This correlates well with their XRD and FT-IR data. The absorption bands at 223 nm, 250 nm, and 311nm due to σ→σ*; n→π*, and π→π* transitions in the aromatic ring [21-22]. However, in current study, we will focus on the largest band (311 nm) of composite (π–π* electronic transitions of the $C_{16}H_{14}O_4$ molecule). This electronic absorption corresponds to transition from the ground state to the first excited state, and is mainly due to an electron excitation from the HOMO to the LUMO. This type of transition occurs in the unsaturated centers of the molecules, i.e. in compounds containing double or triple bonds, and in aromatics compounds. In the near UV region of the spectra, bands observed are

called Soret-band (B-band).These could arise from the transitions of a_{2u} (π) highest occupied molecular orbital (HOMO) to e_g (π^*) lowest unoccupied molecular orbital (LUMO) [21-22].

Fig.(4) shows the UV-VIS absorption spectra of PVA/ $C_{16}H_{14}O_4$ films after γ irradiations. After irradiation, there is a decrease in the absorbance coefficient (Fig.4) and also a small shift in band edge. A small broadening of the peaks can also observed, and this could be due to the production of radiation induced defects which lead to the formation of new energy levels, causing the peak broadening in system. Another, possible cause may be the excitation of non bonding electrons generated by the presence of structural defects (due to the creation of free radicals or ions) into the conduction band , in addition to their localized states [19-20, 24-27]. The increase of carriers on localized states due to the formation of free radicals or ions will give rise to reduction in the transition probabilities into the next extended states, and there causing additional absorption [24-27].Various irradiation studies also confirms the increase in absorbance, due to the formation of new chemical species, caused by energy transfer by the incident radiations [19-20].

The optical energy gap of these irradiated samples was calculated by using the well known Tauc equation [28]:

$$\alpha h\upsilon = B(h\upsilon - E_g)^n \qquad \ldots(1)$$

where "α" is absorption coefficient, "$h\upsilon$" is the energy (h is a Planks constant having value 6.625 x 10^{-34} J/s and υ is the frequency of incident photon in Hz) of the incident photon, E_g is the value of the optical band gap and "*n"* is the exponent indicating the type of electron transition in the system. Generally, n takes values 1/2 and 2 for direct allowed and indirect allowed transitions respectively. Also, the factor B is constant and depends on the transition probability.

According to our previous optical absorption studies on similar compounds[], these materials are found to follow indirect allowed transitions. Hence Tauc plots are drawn between $(\alpha hv)^2$ versus hv. Fig. 5 shows the Tauc plots of the investigated composite films. After irradiations, a slight increase in E_g (red shift) is observed with increase in dose (up to 30Gy) (see Table II). However, in 50Gy irradiated sample, E_g is reduced drastically than the pristine. There are number of reports on different aromatic systems, where a decrease in band gap after irradiation was observed [19-20, 29]. It is argued that the decrease in band gap after irradiation produces defects, such as radicals, cations, anions, etc in the material which increase the disorder and causing the structural deformation in the system [24-27]. Also according to the density of state model, E_g decreases with increasing the degree of disorder of the amorphous phases [28]. A similar trend in E_g after gamma irradiations in other polymers was also observed [24-25]. This observed variation of band gap is consistent with the variation in dielectric of the current system (will be discussed in later section).

The Urbach band tail (also called defect tail) was also studied in these composites. This Urbach energy is used to study subgap absorptions in details. The Urbach energy (E_u) was determined using Urbach rule [28]:

$$\alpha = \alpha_0 \exp(h\upsilon)/ E_u \qquad ..(2)$$

where α_0 is the pre-exponential absorption coefficient factor. It may be noted that the various factors like the carrier phonon interaction, carrier-impurity interaction and structure disorder are main reasons for the Urbach band tail in semiconductors [20, 22,24]. By fitting equation (2), the values of E_u are determined from the inverse slope of the straight line, representing $ln(\alpha)$ versus photon energy ($h\upsilon$). There is a slight decrease in E_u with dose (Table II). But at the highest dose, an increase in this parameter is observed (Table II). Therefore, as E_g increases, the magnitude of

defect energy decreases. However, with highest dose, sub-band states formed in between the valence and conduction band may lead to the narrowing of E_g. Also, the number of defect levels below the conduction band increases to such an extent that the band edge is shifted deep into the forbidden gap, thereby reducing the effective E_g of present system. Hence, it clearly demonstrated that the enhancement in existing defects or disorder after irradiation may be the prime reason for this observed behavior. It should be also noted that during irradiations, there are release of gases from the polymeric material. These released gases are mostly, H, H_2, CO, or CO_2 and can led to the carbonaceous clusters in the polymer matrix. These carbonaceous cluster (being rich charge carriers) impacts the various physical properties of the polymeric material.

3.4. Dielectric Studies

The dielectric constant (ε_r) can be calculated by the following equation:

$$\varepsilon_r = Cd/\varepsilon_0 A \qquad \text{--- (3)}$$

where C is the capacitance (F), ε_0 is the free space dielectric constant value (8.854×10^{-12} F/m), A is the capacitor area (m^2) and d is the thickness (m) of the material.

The imaginary part of the dielectric constant (ε_i) or loss was calculated using the following relation

$$\varepsilon_i = \varepsilon_r tan\delta \qquad \text{--- (4)}$$

where tanδ is the dielectric loss. From the ε_r and ε_i the *ac* conductivity (σ_{ac}) of the present sample was calculated using the following relation [30]:

$$\sigma_{ac} = \omega\, \varepsilon_r\, \varepsilon_0\, tan\delta \qquad \text{--- (5)}$$

where ω is the angular frequency.

Also σ_{ac} obeys the following power law [30]:

$$\sigma_{ac}(\omega\ T) = B\omega^{s} \qquad \text{--- (6)}$$

where B and s are the composition and temperature dependent parameters respectively. Here s takes value between "0" and "1". When $s = 0$, the electrical conduction is frequency independent, like dc conduction at very low frequencies, and when $s > 0$, the conduction is frequency dependent or *ac* type [30].

Fig. 6 shows the variation of the ε_r as a function frequency (120-500kHz) irradiated with different doses. At first look, all films show a random variation in the ε_r with dose (decreases for 15 Gy then increases till 50Gy). The observed behavior, like decrease of ε_r with frequency can be due to the contributions of various factors like polarizability, deformation and relaxation. PVA is a solid semicrystalline dielectric material containing polar groups. The main contribution of polarizations comes from ionic, space charge and orientation because of the presence of free ions and polar molecules in this type of materials. Also, in such polymers, the polarizations like electronic polarization caused by deformation of the electronic shells and appearance of induced dipoles are low. However, the addition of plant molecules in PVA films and then irradiations may would have affected the dipoles (by formation of defects and free radicals etc) and altered the dielectric properties. By increasing the applied frequency, the dipoles will no longer be able to rotate much quickly. Hence, their oscillations begin to lag behind the applied field (frequency). Also when the frequency is further increased, the dipoles will completely be unable to follow the applied field and the orientated polarization vanishes. This cause decrease in ε_r and

attains a constant value at higher frequencies. For all the samples, as evident from plots, the ε_r shows a well dispersion over entire range of frequencies (120-500kHz). Generally in the irradiated polymers, fluctuations in ε_r can be observed [25]. Also at higher frequencies, the charge carriers get trapped at defect sites causing neutralization of charges there, and hence leading to the decrease in the observed ε_r [25,29]. Also the ε_i of pristine (0Gy) and irradiated films decreases at lower frequencies (2kHz for 0Gy, 6kHz for 15Gy,1.9KHz for 20Gy, 6.2kHz for 30Gy, and 9.6kHz for 50Gy) (see Fig.7). After these frequencies, it starts increasing, then again decreases, and finally showing a relaxer behavior. Generally, this relaxation in pure polymers can be observed at low frequencies (say few 100Hz's). But the higher value observed here in pristine could be due to composite formations. One of the possible reasons for this observed behavior is that the polymer may develop a network structure after irradiation. The movement of chain segments is getting reduced due to the scissions resulting low dipole oriented polarizations [25,29]. However, with the enhancement of radiation dose, random breaking of bonds might have taken place. This can increase the degradation process of polymer. This degradation creates lesser number of entanglements per molecule, thereby increasing the chain mobility, and hence increases the ε_r and ε_i [29]. In most polymers, radiation can also increases the number of C=O and C=C bonds in the polymer matrix. Furthermore, the weaker C=C bonds may become a source of free carriers under the influence of *ac* field (or bias) [31], and affecting the dielectric properties of material. The another possible reason for variation in dielectric properties is related to the presence of C-C, and C=O bonds in the irradiated samples, which is obvious from the following ratios: $\alpha_p(C=C)/\alpha_p(C–C)= 2.99$, α_p (C=O)/ α_p (C–C) = 2.06 and in which αp(C–C), αp(C=C), αp(C=O) represent components of the polarizability parallel to C–C, C=C, and C-O bonds, respectively[32].

Fig.(8) shows the variation of ln(σ_{ac}) versus ln(ω) for all the under study samples. It is observed that the *ac* conductivity increases steeply up to certain frequency and then decreases. This observed trend is a general feature of disordered or inhomogeneous materials. The present system follows the universal law behaviors described by eq.(6). In order to examine the nature of charge carrier hopping in the under study materials, the exponent "*s*" was calculated by plotting ln(σ_{ac}) versus ln(ω) (see Fig.8). There the frequency exponent *s* was computed from the slope of the straight lines where $s = \partial\sigma_{ac}/\partial\omega$. In the present study, after irradiations the value *s* lie between 0.99 to 0.89, suggesting that the conduction phenomenon in the current composites is *ac* type and are due to the hopping of charge carriers [30].

It is a well established fact that polymer structures are mostly disordered materials (or heterogeneous microstructure). For such type of systems, frequency dependent dielectric data can be explained in view of universal dielectric response (UDR) model [30,33]. In view of this model, localized charge carriers are hopping among spatially fluctuating lattice potentials, producing the charge transport. Also, these fluctuations can further induce dipolar effect. To study our system more vividly, we have analyzed our data according to universal dielectric response (UDR) model. For our samples, we got a linear behavior in the log (f .ε_r) versus log (f) plots throughout studied frequency range (see Fig.9). It means that UDR phenomenon is responsible for dielectric response of these samples. In the current samples, one can notice a dramatic effect on various physical properties at 15Gy dose. Beyond this dose, unsystematic change in these physical properties is observed. Therefore, to explore these films below 15Gy, more detailed experiments are under way.

4. Conclusion

Composite thin films of Coumarin and PVA were prepared and exposed to γ-ray irradiation at room temperature. These as prepared films are characterized by various techniques before and after irradiations. Molecular vibrations and associated bands are studied by FTIR spectroscopy. Impact of radiation on different bands are observed and discussed. This system exhibits a strong optical absorption at 311nm. Band gap analysis is carried out this band and this composite follows indirect allowed transition. Radiation modifies various optical parameters like E_g and E_u and these optical parameters are directly related to radiation induced disorder or creation of defects in the system. The ε_r and ε_i show dispersion in the lower frequency region for all the samples. The *ac* conductivity obeys the Jonscher's power law: $\sigma_{ac}(\omega) \sim \omega^s$. The electrical transport mechanism in the present films is due to the hopping of charge carriers. These thin films follow the UDR model and indicate a strong disorderness in these films before and after irradiation. However, additional studies are still required to evaluate the optimum dose for this system.

Acknowledgments

One of the authors (FAM) thanks DST (India) for providing him Fast Track Young Scientist project (SR/FTP/PS-148/2012). He also thanks the Director, IUAC for support.

References

[1] H.M. Khan, M. Anwer, Z.S. Chaudhry, Rad. Phys. Chem. 63, 713–717,(2002).

[2] Z. Ajji, Rad. Meas. **41**, 438–442 (2006).

[3] J.A. LaVerne, L. Tandon, B.C. Knippel, V.M. Montoya, Rad. Phys. Chem. **72**, 143–147(2005).

[4] D.V. Parwate, I. D. Sarma, R.J. Batra, Rad. Meas. 42, 1527–1529(2007).

[5] H.M. Khan, S.Naz, Nucl. Sc. Tech. **18**, 141–144(2007).

[6] A. CHAPIRO, Radiation Chemistry of Polymeric Systems, Interscience Publishers, 1962

[7] M.F. Barakat, K. El-Salamawy, M. El-Banna, M.A. Hamid, A.A.R. Taha, Rad. Phys. Chem. **61**, 129–136(2001).

[8] M. A. Rauf, S. S. Ashraf, J. Haz. Mat. **166**(1), 6-16(2009).

[9] H.H. Mai, H.M. Solomon, M. Taguchi, T. Kojim, Radiation Physics and Chemistry 77 (2008) 457–462.

[10] A. Moussa, M. Baranyai, L.Wojnarovits, A. Kovacs,W.L. McLaughlin, Radiation Physics and Chemistry 68 (2003) 1011–1015.

[12] A. Akhavan, M. Sohrabpour, M. Sharifzadeh, Radiation Physics and Chemistry 63 (2002) 773–775.

[13] O. R. Kennedy, R. D. Thornes,. In Coumarins: Biology, Applications and Mode of Action; Wiley and Sons: Chichester 1997.

[14] A. K. Collins, G.M. Makrigiorgos, G.K. Svensson,. Med. Phys. **21**(11), 1741–1747 (1994).

[15] K. Gopakumar, U.R. Kini,., S.C. Ashawa, N.S. Bhandari, G.U. Krishnan, D Krishnan, Radiat. Eff. Defects Solids **32** (3-4), 199–203, (1977).

[16] Y. Manevich, K. Held, J.E. Biaglow, Radiat. Res. **148**, 580–591 (1997).

[17] M. A. Park, , S.C. Moore, N. Limpa-Amara, Z. Kang, G.M. Makrigiorgos, Nucl. Instrum. Methods Phys. Res. Sect. A—Accel. Spectrom. Dect. Assoc. Equip. **569**(2),543–547 (2006).

[18] G.M. Makrigiorgos, J. Baranowskakortylewicz, E. Bump, S.K. Sahu,., R.M. Berman, A.I. Kassis, Int. J. Radiat. Biol. **63** (4), 445–458 (1993).

[19] F. A. Mir, S.Rehman, and S.H.Khan, Nucl. Rad. Phys. **68**, 21921-21922 (2014).

[20] F. A. Mir, S. A. Rather, J. A. Banday and S. H. Khan, Radiat. Eff. Defects Solids, **169**, 11, 906–912 (2014).

[21] J. A. Banday, F. A. Mir, M. A Qurishi, S. Koul, and T. K. Razdan J. Therm. Anal. and Cal. **112**:1165–1170 (2013).

[22] F.A. Mir, Appl. Phys. A **120**:1659–1663(2015).

[23] J. Tripathi, S. Tripathi , J.M. Keller, K. Das, T. Shripathi, Polymer Degradation and Stability **98** , 12-21, (2013).

[24] K. Sharma, R. P. Chahal, S. Mahendia, A. K. Tomar, S. Kumar, Radiat. Eff. Defects Solids, **168**, 5, 378–384 (2013)

[25] D. Fink, Fundamentals of Ion-Irradiated Polymer; Springer-Verlag: Berlin, Heidelberg, 2004.

[26] Shu-Juan Zhang, Han-Qing Yu, Water Research, **38**, 309–316(2004).

[27] N. M. El-Sawy, M. B. El-Arnaouty, A. M. A. Ghaffar, Polymer-Plastics Technology and Engineering, **49**: 169–177 (2010).

[28] N. F. Mott, & E. A. Davis, Electronic process in non-crystalline materials (2nd ed.). UK: Clarendon press Oxford, 1979.

[29] Z. Qi, B. Wei, Y. Sun,. X. Wang, F.Kang, M. Hong, L.Tang, Polym. Bull., **66**, 905 (2011).

[30] A. K. Jonscher, Dielectric Relaxations in Solids , Chelsea Dielectrics Press, London, 1983.

[31] B. S. Rathore, M. S. Gaur, F. Singh and K. S. Singh, Radiation Effects & Defects in Solids, **16**, 72, 131–140 (2012).

[32] M. Šiljegović , Z. M. Kačarević-Popović, M. Stchakovsky, A. N. Radosavljević, S. Korica, M. Novaković, M. Popović, Radiation Physics and Chemistry, **98**, 7–13(2014)

[33] C. R. Bowen and D. P. Almond, Materials Science and Technology, **22**, 6 ,719 (2006).

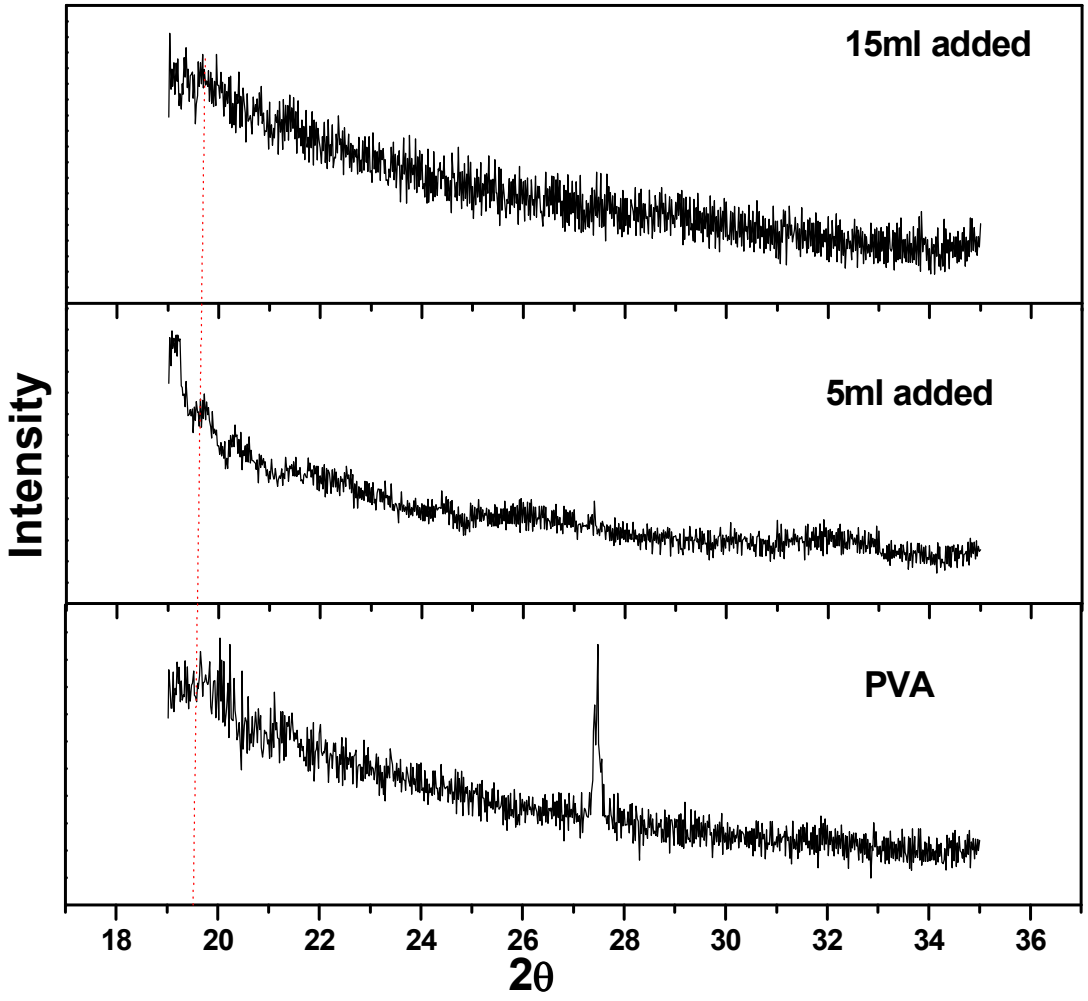

Fig.1. XRD pattern **of PVA and composite films with different Imperatorin concentrations.**

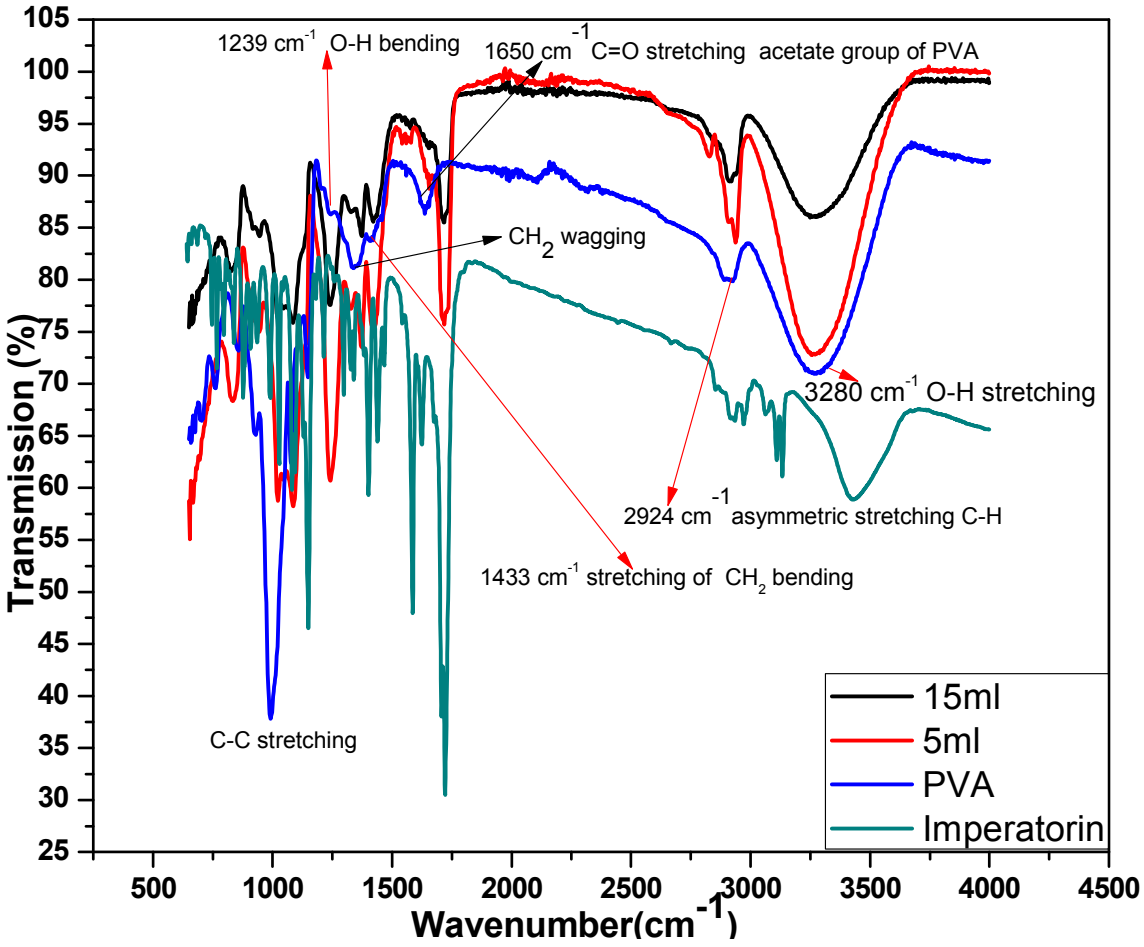

Fig.2. FT-IR spectrum of PVA, Imperatorin, composite films with different Imperatorin concentrations.

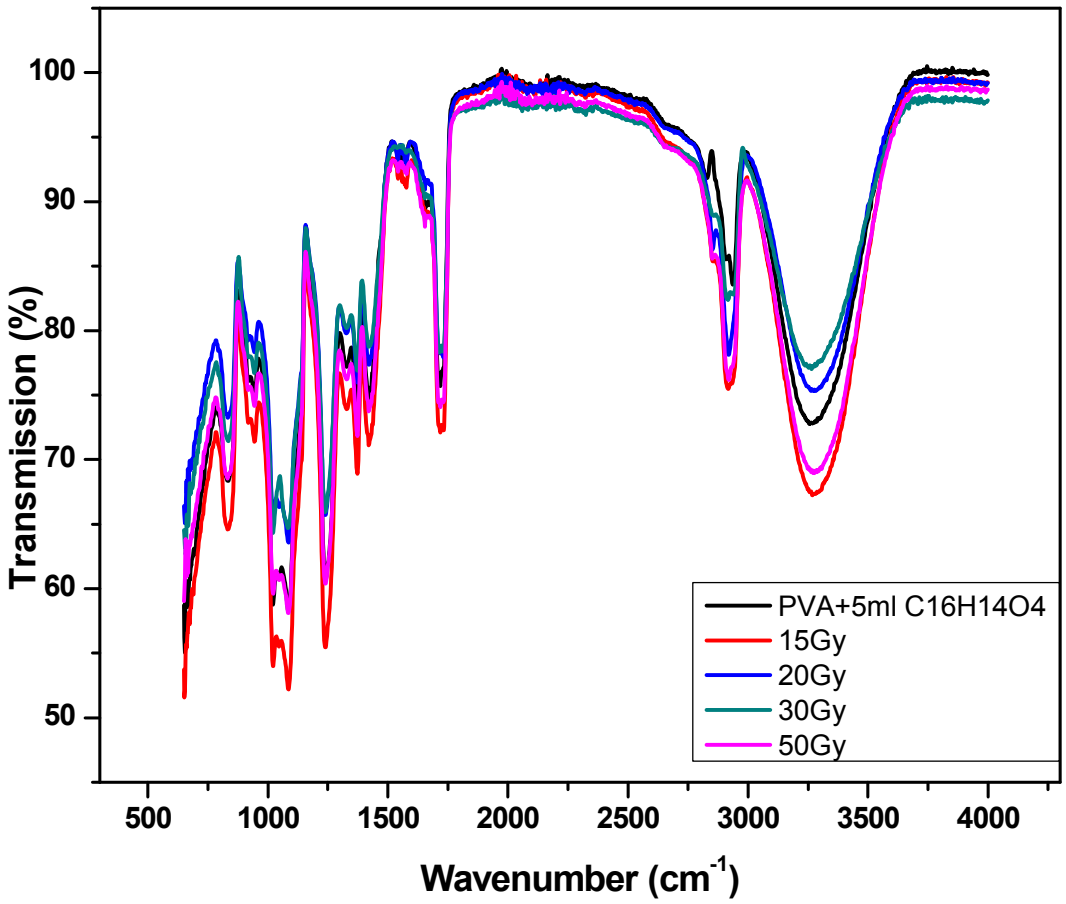

Fig. 3. FT-IR spectrum of pristine and composite films after irradiation.

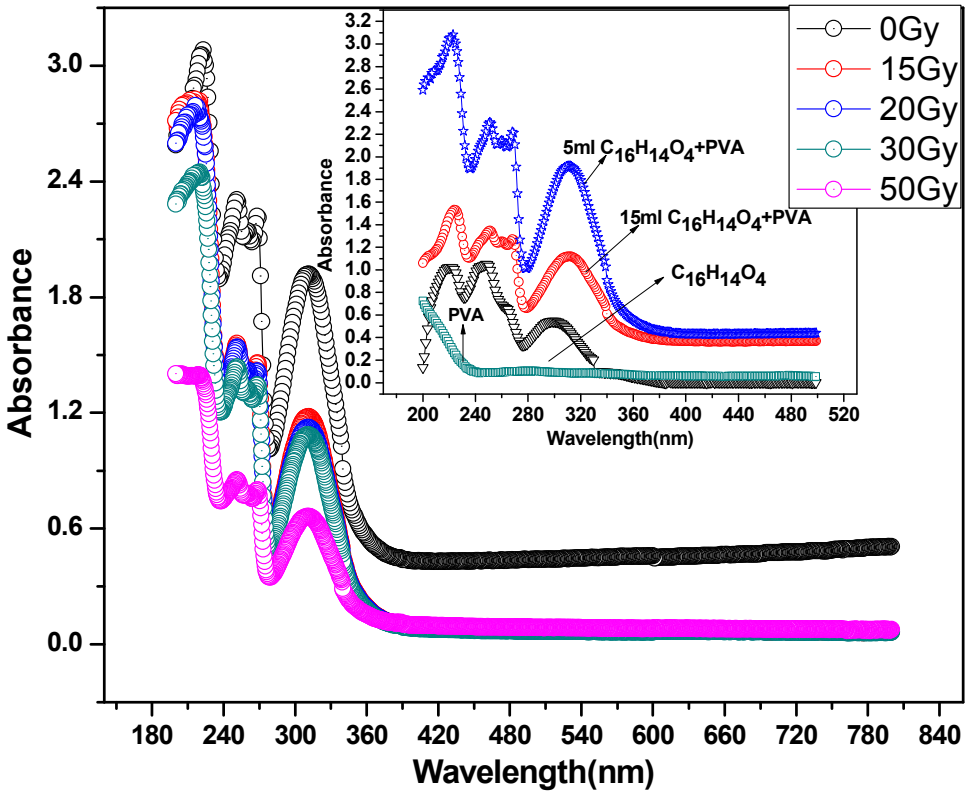

Fig.4. UV–Vis spectrum of composite films irradiated at 0,15,20, 30, and 50 Gy doses. Inset shows UV–Vis spectrum of PVA, $C_{16}H_{14}O_4$, 5ml , and 15 ml $C_{16}H_{14}O_4$+PVA composite films.

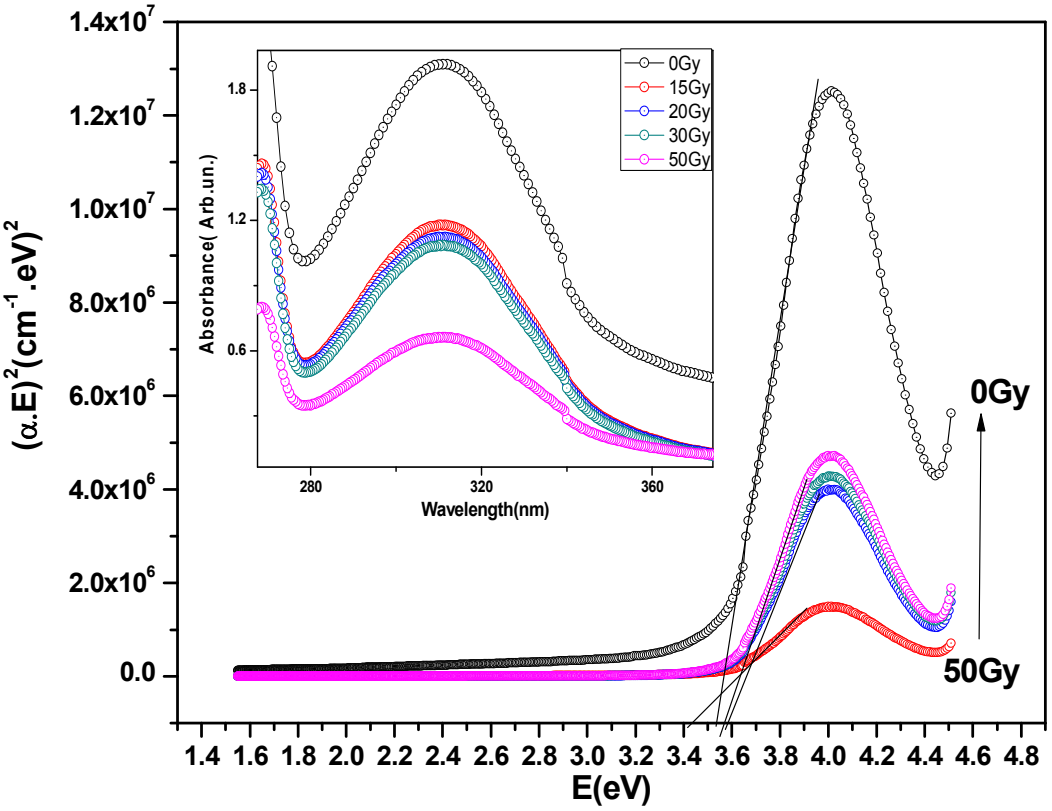

Fig.5. Tauc plots for band gap calculation for these composite films irradiated at 0,15,20, 30, and 50 Gy doses. Inset shows enlarged view of 311nm band of these films.

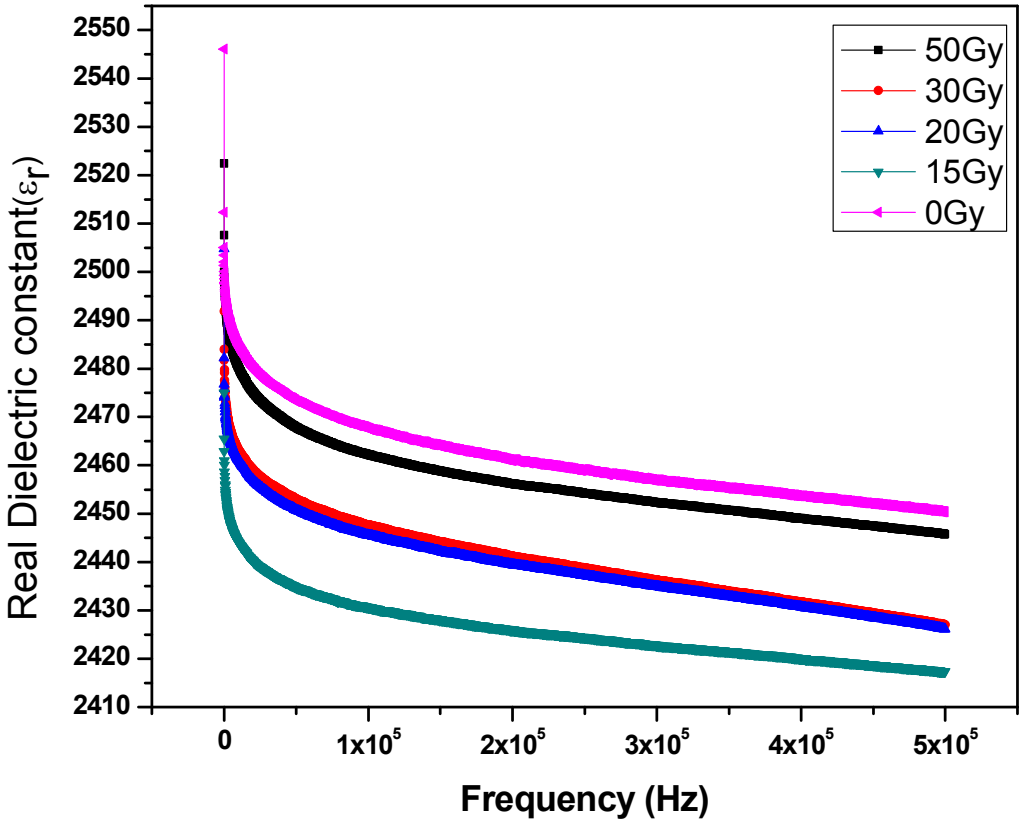

Fig.6. Variation of real dielectric constant with frequencies irradiated at 0,15.20,30, and 50Gy doses.

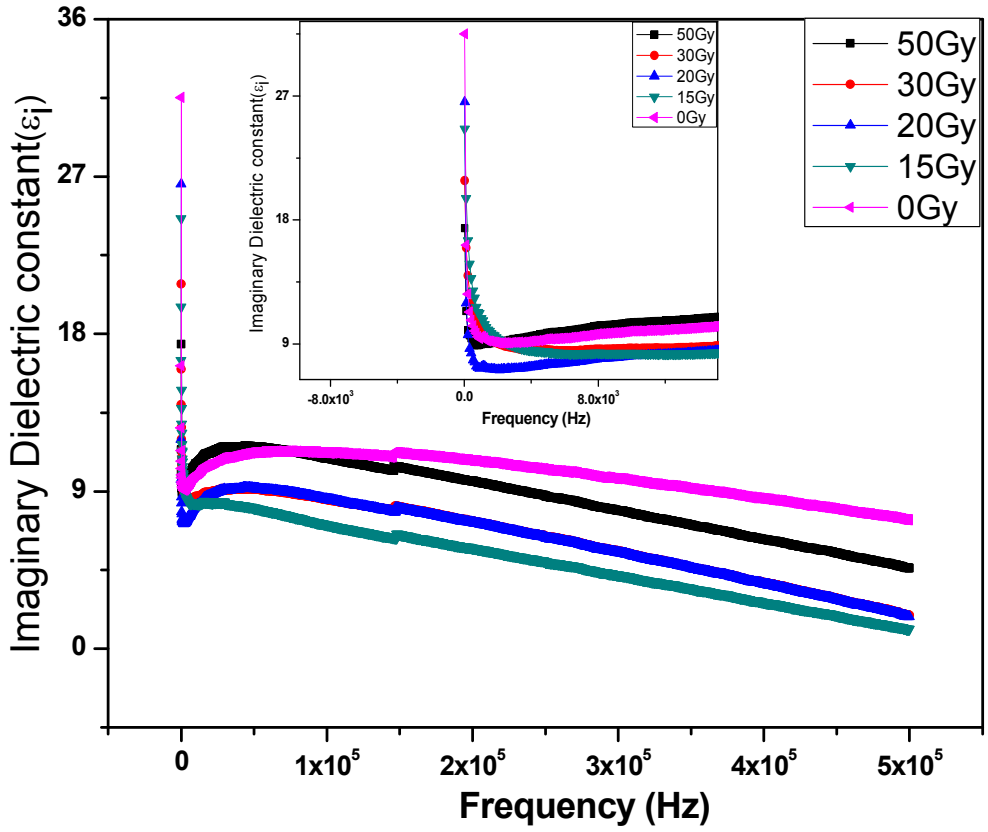

Fig.7. Variation of imaginary dielectric constant with frequencies irradiated at 0,15.20,30, and 50Gy doses. Inset shows plots of these films at low frequencies.

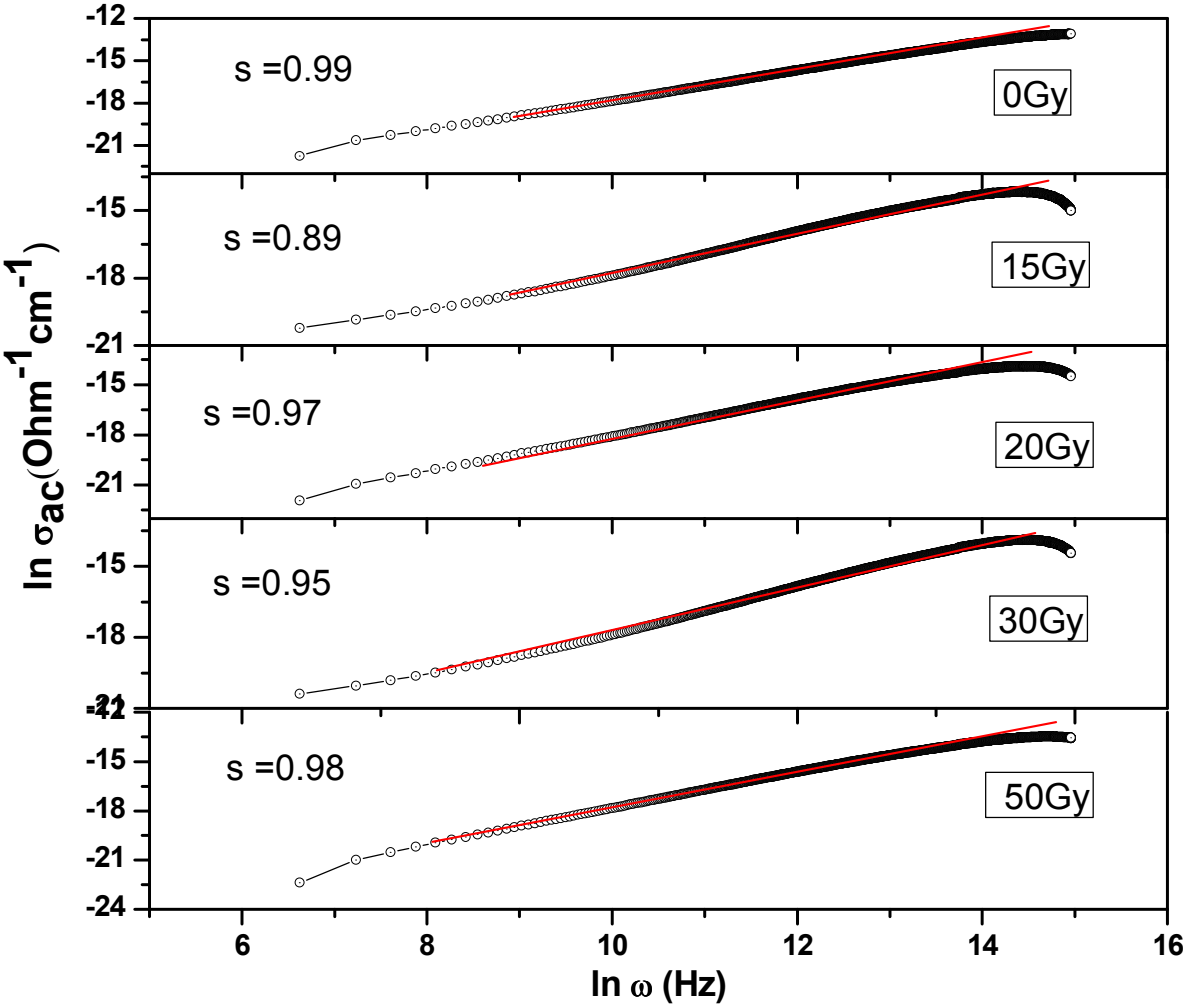

Fig.8. ln (σ_{ac}) versus ln (ω) plots for 0,15.20,30, and 50Gy dose irradiated composite films.

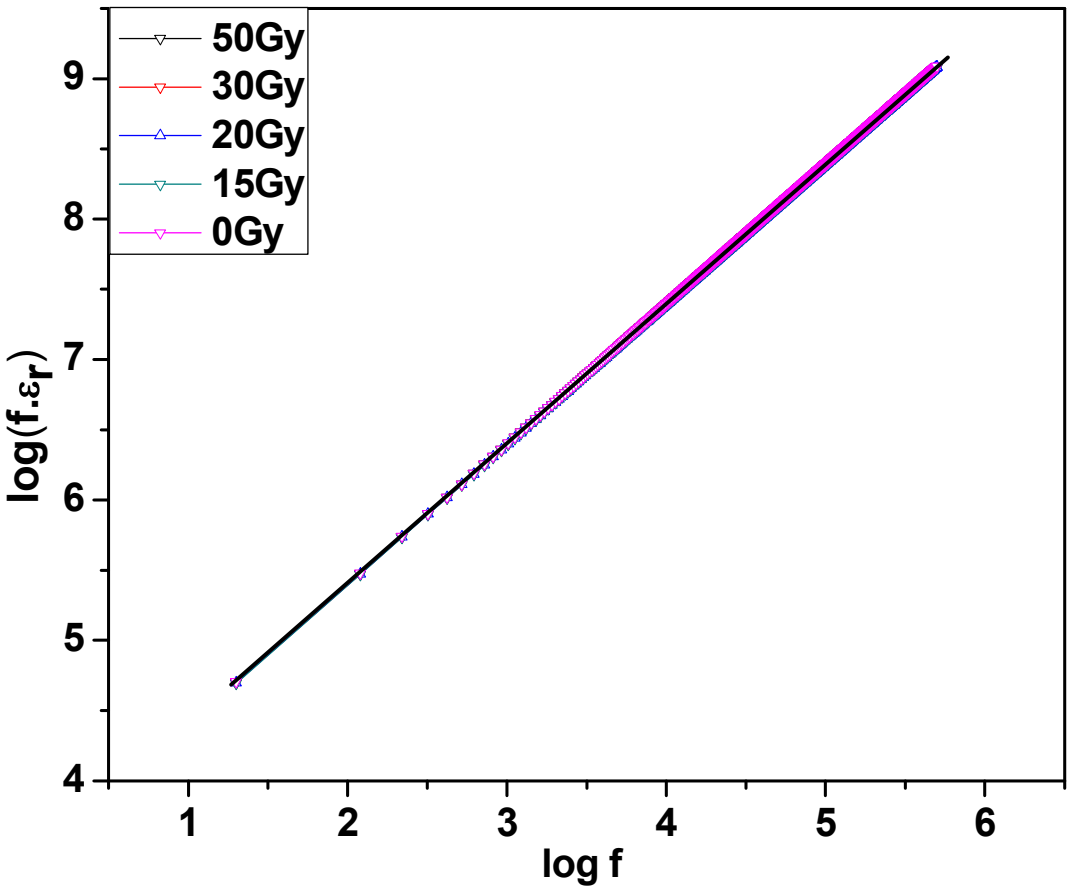

Fig. 9. Alteration of log ($f.\varepsilon_r$) with log (f) for 0,15,20,30, and 50 Gy samples in the frequency range of 120Hz–500kHz.

Table.I Main FT-IR peaks of PVA, imperatorin, and PVA/Imperatorin composite films.

PVA		Imperatorin (or $C_{16}H_{14}O_4$)		Observed bands in PVA/Imperatorin Composite
Wavenumber (cm^{-1})	Assigned vibrational bands	Wavenumber (cm^{-1})	Assigned vibrational bands	Wavenumber (cm^{-1})
3700-3000	O-H stretching	2,966	Asymmetric C–H stretching	33679-2988
2920	C-H symmetric stretching	2,852	Symmetric C–H stretching	2929
1720	Carbonyl (C=O)stretching	1,460	Asymmetric –CH3 bending	1738
1645	Acetyl (C=C) stretching	1,375	Symmetric –CH3 bending	1722
1430	CH_2 bending	3,133	Aromatic C–H stretching	1422
1370	CH_2 wagging	1,150	C–O stretching	1371
1250	C-H wagging	1,722	α,β-unsaturated-δ-lactone	1241
1100	C-O stretching	3,427	C–C–O' symmetric stretching	1086
937	C-C stretching	1,586	Aromatic C–C stretching	947
855	CH_2 stretching	1,401		834
627	O-H stretching	877	Olefinic C–H out of plane bending	657
		745	Aromatic out of plane –C–H bending	
		1,028	Aromatic in of plane –C–H bending	

Table II. Various optical parameters for these irradiated films.

Dose(Gy)	E_g(eV)	E_u(meV)
0	3.53	456
15	3.55	272
20	3.56	275
30	3.57	274
50	3.40	387

"Gamma Irradiation Studies of Composite Thin Films of Poly Vinyl Alcohol and Coumarin"

By

Feroz A. Mir, Adil Gani and K.Asokan

Graphical Abstract